High-resolution two-photon spectroscopy of a $5p^5 6p \leftarrow 5p^6$ transition of xenon

Emily Altiere,[1] Eric R. Miller,[2] Tomohiro Hayamizu,[2] David J. Jones,[1] Kirk W. Madison,[1] and Takamasa Momose[1,2]
[1]*Department of Physics and Astronomy, University of British Columbia, Vancouver, Canada V6T 1Z1*
[2]*Department of Chemistry, University of British Columbia, Vancouver, Canada V6T 1Z1*

(Received 13 October 2017; published 16 January 2018)

We report high-resolution Doppler-free two-photon excitation spectroscopy of Xe from the ground state to the $5p^5(^2P_{3/2})6p\ ^2[3/2]_2$ electronic excited state. This is a first step to developing a comagnetometer using polarized ^{129}Xe atoms for planned neutron electric dipole moment measurements at TRIUMF. Narrow linewidth radiation at 252.5 nm produced by a continuous wave laser was built up in an optical cavity to excite the two-photon transition, and the near-infrared emission from the $5p^5 6p$ excited state to the $5p^5 6s$ intermediate electronic state was used to detect the two-photon transition. Hyperfine constants and isotope shift parameters were evaluated and compared with previously reported values. In addition, the detected photon count rate was estimated from the observed intensities.

DOI: 10.1103/PhysRevA.97.012507

I. INTRODUCTION

Work is underway on a next generation neutron electric dipole moment (nEDM) measurement at TRIUMF's ultracold neutron (UCN) facility in Canada [1]. The best nEDM measurement, to date, comes from the RAL-Sussex-ILL Collaboration with an upper limit of $|d_n| < 3.0 \times 10^{-26} e$ cm [2]. This previous experiment used a ^{199}Hg comagnetometer to correct for the drifts in the applied magnetic field. However, the precessing ^{199}Hg atoms acquire an additional phase from geometric phase effects (GPE) as they move about in the magnetic field gradient [3], which imparts a residual systematic error on the $|d_n|$ measurement.

The UCN Collaboration at TRIUMF is preparing to employ a ^{129}Xe/^{199}Hg dual species comagnetometer [4]. The two cohabiting systems will enable simultaneous measurements of both the magnitude and gradient of the magnetic fields, thereby reducing the systematic error due to magnetic field inhomogeneity in the nEDM measurement down to $<10^{-27} e$ cm. ^{129}Xe is a potential comagnetometer species because it possesses nuclear spin ($I = 1/2$) and has a neutron capture cross section two to three orders of magnitude less than that of ^{199}Hg [5]. There are other possible atomic candidates, such as ^{3}He [6]; ^{129}Xe was selected by the UCN Collaboration because the optical excitation and detection scheme is compatible with the ^{199}Hg system, both with accessible excitations in the deep UV. In order to detect the ^{129}Xe precession, we will use two-photon excitation [7], with optical detection via laser-induced fluorescence (LIF) [4]. Optical detection is sensitive to the nuclear polarization when using circular polarized light to excite the ground state under a specific geometry, as the selection rules only allow for excitation from a single Zeeman sublevel.

We plan to use the $5p^5(^2P_{3/2})6p\ ^2[3/2]_2 \leftarrow 5p^6\ (^1S_0)$ two-photon transition to detect the precession between Zeeman-split ground-state sublevels of polarized ^{129}Xe atoms. In this paper, we present the results of the hyperfine-resolved high-resolution spectroscopy of this transition with 252.5 nm photons. From this excited state, we detect LIF to the $5p^5 6s$ intermediate state for the six most abundant Xe isotopes (see Fig. 1, inset, for the energy diagram). Based on the transition frequencies calibrated by a self-referenced frequency comb [8], we derived the hyperfine constants for ^{129}Xe and ^{131}Xe, and the isotope shifts between spectral peaks. We also estimated the photon count rate detected on an avalanche photodiode (APD) for the transition.

Early measurements of hyperfine structure and isotope shifts were performed for many Xe levels using discharge sources [9–11] and magnetic resonance in atomic beams [12]. Doppler-free spectroscopy using saturated absorption and crossed-beam methods enabled improved measurements between various excited levels [13–15]. Doppler-free spectroscopy from the ground state has also been observed using two-photon excitation [16–18], but no high-resolution spectroscopy has been reported on the transition we are investigating.

Previous work on the determination of hyperfine constants of Xe was done by detecting hyperfine structures in transitions between two states, both with their own hyperfine manifold. In the present work, we excite directly from the ($J = 0$) ground state, and therefore the hyperfine constants of the $5p^5(^2P_{3/2})6p\ ^2[3/2]_2$ excited state were determined directly.

II. EXPERIMENTAL SETUP

The $5p^5(^2P_{3/2})6p\ ^2[3/2]_2 \leftarrow 5p^6\ (^1S_0)$ transition, described using the Racah notation of [19], requires two photons at 252.5 nm. Recent developments in semiconductor laser technology have made available high-power sources in the near infrared (NIR) suitable to generate substantial power in the ultraviolet (UV) via two stages of second harmonic generation (SHG). In this experiment an optically pumped semiconductor laser (OPSL) at 1010 nm was used. This type of continuous wave laser is optimal because of its narrow linewidth, <100 kHz, and high power of 3 W. The 1010 nm light is then frequency doubled to 505 nm using a lithium

 ©2018 American Physical Society

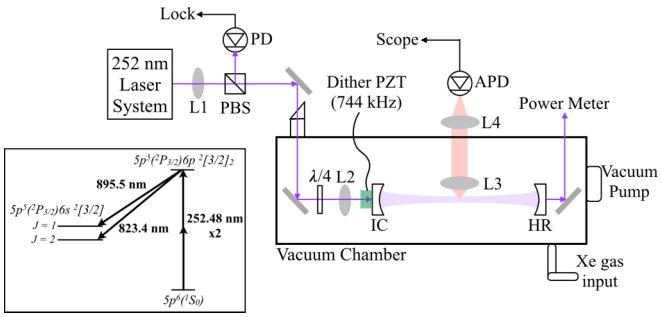

FIG. 1. Experimental setup of the UV enhancement cavity in the vacuum chamber, backfilled with Xe and O_2 gas. The cavity is made with two curved mirrors, an input coupler (IC) and high reflector (HR), each with radius of curvature = 150 mm and separated by 260 mm. L1 and L2 are lenses for mode matching the UV light into the enhancement cavity. A quarter wave plate ($\lambda/4$), a polarized beam splitter (PBS) and a piezoelectric transducer (PZT) are used to lock the UV cavity. We collect fluorescence perpendicular to the beam at the focus of the cavity using two 1 in diameter lenses, L3 and L4, with focal lengths 19 mm and 50 mm, respectively. The light is focused onto an APD placed outside the vacuum chamber. A power meter monitors the circulating UV power. Inset: relevant energy levels corresponding to the two-photon transition and LIF under investigation.

triborate (LBO) nonlinear crystal followed by a second doubling stage with a beta barium borate (BBO) nonlinear crystal to 252.5 nm. Enhancement cavities, with a bowtie configuration, were used for the frequency doubling stages to maximize the SHG conversion. Prior work on the OPSL and SHG in this configuration can be found in Ref. [20].

Following the two SHG stages, the UV light was coupled into a Fabry-Perot enhancement cavity. The two curved mirrors (radius of curvature = 150 mm) separated by 260 mm enhance the UV power for the two-photon absorption. The cavity geometry and optics were selected based the size of the UCN bottles (radius ~200 mm) at TRIUMF. Additionally, the cavity provides retroreflection of the beam, which enables Doppler-free two-photon spectroscopy with counterpropagating photons. For this experiment, the UV cavity enhanced the 40 mW output of the second SHG stage by five times, yielding a circulating power of 200 mW. The Fabry-Perot cavity was built inside a vacuum chamber that was evacuated and backfilled with 1.6 Torr total pressure of Xe and O_2 gas at a 50:50 ratio. The partial pressure of O_2 was introduced to maintain the finesse of the cavity inside the vacuum chamber during the spectroscopy measurements. We suspect that UV photolysis of O_2 removes residual gases deposited on the dielectric mirrors, which spoil the cavity finesse. We measure with an APD both 895 nm and 823 nm fluorescence transmitted transverse to the beam from the excited state via the transitions $5p^5(^2P_{3/2})6p\ ^2[3/2]_2 \rightarrow 5p^5(^2P_{3/2})6s\ ^2[3/2]_{J=1,2}$. An APD was selected for its convenient spectral sensitivity ranging from 600–950 nm and peaking at 800 nm. Two lenses were used to collect and maximize the emitted light from the focus of the cavity onto the APD. A schematic of the apparatus is shown in Fig. 1.

We tune the frequency of the laser by applying a driving voltage to a piezoelectric transducer mounted to the output mirror, changing the cavity length of the OPSL. The doubling cavities are locked to the laser and thus track this frequency. We scan the laser frequency by 400 MHz in the NIR. This corresponds to 3.2 GHz in the Xe transition frequency spectrum, eight times larger due to the two SHG stages and the two-photon excitation. The frequency of the OPSL is monitored during the scan by recording the heterodyne beat spectrum between the NIR light and a fiber-based self-referenced frequency comb described in Ref. [8].

III. RESULTS AND DISCUSSION

The ^{129}Xe and ^{131}Xe isotopes experience hyperfine splitting as a result of their nonzero nuclear spin, $\boldsymbol{I}$. By adding the electronic angular momentum $\boldsymbol{J}$ with the nuclear spin we can write the total angular momentum as $\boldsymbol{F} = \boldsymbol{J} + \boldsymbol{I}$. The hyperfine interaction between the electronic angular momentum and the nuclear spin leads to an energy shift and splitting. To second order this can be approximated by magnetic-dipole and electric-quadrupole interactions [21]. The peak positions for the odd isotopes can then be written as

$$\nu_i(I,J,F) = \nu_{0,i} + A_i\frac{K}{2} + B_i\frac{\frac{3}{2}K(K+1) - 2I(I+1)J(J+1)}{4I(2I-1)J(2J-1)}, \quad (1)$$

where

$$K = F(F+1) - I(I+1) - J(J+1), \quad (2)$$

$\nu_{0,i}$ is the center of gravity of isotope i (i = 129 or 131), and A_i and B_i are the magnetic-dipole and electric-quadrupole hyperfine constants, respectively. The even isotopes of Xe all have zero nuclear spin and are therefore free of hyperfine structure. In the case for ^{129}Xe, the quadrupole term vanishes because $I = 1/2$, leaving only the magnetic-dipole interaction A_{129} term. ^{131}Xe has $I = 3/2$, and therefore has both A_{131} and B_{131} terms.

Figure 2 shows a two-photon excitation spectrum of Xe for all the detected isotopes. In order to identify the transition frequencies, the peaks were each fit with a Doppler-free Lorentzian line shape. The extraction of the hyperfine parameters of ^{129}Xe and ^{131}Xe was combined with the Lorentzian fit using Eq. (1) to simultaneously fit the respective peaks of each isotope. We measure a 59 MHz full width at half maximum linewidth across all peaks. We find no difference in linewidth when fitting with a Voigt profile. Therefore, the dominant contribution to the current linewidth is believed to be pressure broadening followed by lifetime broadening. The observed width is roughly consistent with the pressure broadening of 28.8 MHz Torr^{-1} measured by Plimmer *et al.* [16].

The values of hyperfine constants A_i and B_i are reported in Table I, along with previous experimental measurements for comparison. Since A_i is proportional to the nuclear g factor $g_I = \mu_I/(\mu_N I)$ [21], we can compare directly with values determined via nuclear magnetic resonance. We calculate the ratio $A_{129}/A_{131} = -3.38(1)$, which agrees with the value $g_{129}/g_{131} = -3.375(1)$ calculated from the magnetic moments and spins given in Ref. [22]. The magnetic dipole constants A_i agree well with the previously reported values for both ^{129}Xe and ^{131}Xe shown in Table I. On the other

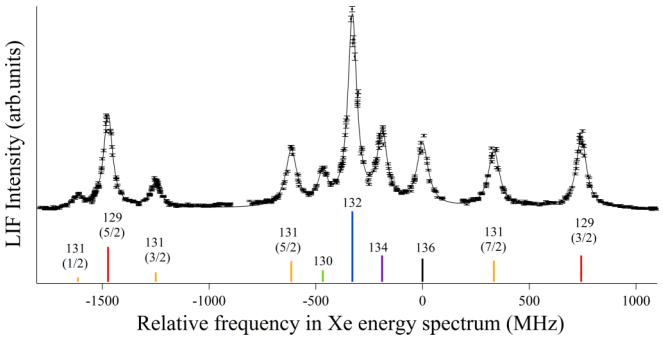

FIG. 2. Excitation spectrum of natural abundance Xe. The total pressure was 1.6 Torr, with a 50:50 ratio of Xe and O_2. The x axis corresponds to the Xe transition frequency, eight times larger than the OPSL frequency. The y axis is the observed LIF intensity of the combined 895 nm and 823 nm emission. The peaks are shown with the fitted Lorentzian line shape as described in the text. Each peak is labeled with its mass number; additionally, odd isotopes are labeled with their excited state hyperfine level F in parentheses. The stick diagram shows the calculated peak positions and intensities obtained from the Lorentzian fit.

hand, the electric-quadrupole term B_{131} is 20%–40% larger than previous measured values. Our determined B_{131} value is expected to be more accurate than the previous values, since it was determined directly from the splitting of the $5p^5 6p$ state, while the previous measurements contain uncertainty from other hyperfine states.

In addition to the hyperfine splitting constants, we calculated the isotope shift of each species relative to ^{136}Xe from their respective peak positions. For the odd isotopes, we used the center of gravity value $\nu_{0,i}$. We report these results in Table II. The isotope shift has two parts: one related to the mass of the nuclei, and a second related to the electric field distribution within the nuclei. By using previously reported values of the change in nuclear charge radius-squared $\delta\langle r^2\rangle$, we fit the observed shift to the following formula:

$$\delta\nu_{i,i'} = K^*\delta\nu_{i,i'}^{NMS} + F^*\delta\langle r^2\rangle_{i,i'}, \tag{3}$$

where $\delta\nu_{i,i'}^{NMS}$ is the normal mass shift between isotopes i and i', given by

$$\delta\nu_{i,i'}^{NMS} = \nu_0\left(\frac{m_e}{u}\right)\left(\frac{i'-i}{ii'}\right). \tag{4}$$

TABLE I. Hyperfine splitting constants (in MHz) for the $5p^5(^2P_{3/2})6p\ ^2[3/2]_2$ excited state of ^{129}Xe and ^{131}Xe. Values obtained by previous works are listed in the last column for comparison. Values in parentheses are the 1σ standard deviation of the last digit.

Hyperfine Splitting Constant	This Work	Previous Works
A_{129}	−886.3(2)	−886.1(8) [13], −889.6(4) [14], −886.2(28)[15]
A_{131}	262.6(10)	263.1(6) [13], 262.7(4) [14], 263.2(13) [15]
B_{131}	34.8(5)	29(2) [13], 21.3(6) [14], 26.8(60) [15]

TABLE II. Isotope shifts $\delta\nu_{136,i'} = \nu_{i'} - \nu_{136}$ of the transition $5p^5(^2P_{3/2})6p\ ^2[3/2]_2 \leftarrow 5p^6\ (^1S_0)$. We follow the sign convention for isotope shift outlined in Ref. [23]. Shifts for the odd isotopes were determined using the center of gravity from the hyperfine splitting. The values of $\delta\langle r^2\rangle_{136,i'}$ are from Ref. [13].

i'	Isotope Shift (MHz)	$\delta\langle r^2\rangle_{136,i'}(fm^2)$ [13]
129	− 586.8(4)	− 0.152(40)
130	− 467.7(5)	− 0.117(40)
131	− 461.2(4)	− 0.124(30)
132	− 326.0(3)	− 0.0844(200)
134	− 187.0(4)	− 0.0518(120)

K^* measures the mass shift and F^* the field shift, ν_0 is the Xe transition frequency, and m_e and u are the electron mass and atomic mass unit, respectively. We fit the observed isotope shifts against published $\delta\langle r^2\rangle$ data sets [13,23,24] to extract values of K^* and F^*. Using the data reported by Borchers *et al.* [13] yields the fit with the smallest uncertainties and the values $K^* = 0.36(2)$ and $F^* = 2640(80)\,\mathrm{MHz\,fm^{-2}}$. A clearer comparison was facilitated by subtracting off the mass shift from the isotope shift, using the respective fit parameters for K^* and F^*, leaving only the field shift term. From this we performed a linear fit of field shift vs. $\delta\langle r^2\rangle$ as shown in Fig. 3, and calculated the mean squared error (MSE) from the residuals shown in the inset of Fig. 3. We calculate the MSE values 1.7 MHz for Borchers' data, and 38.8 MHz and 57.9 MHz for Aufmuths' and Fricke's data, respectively. This indicates that our observed isotope shifts are consistent with Borchers' values of $\delta\langle r^2\rangle$. We find similar agreement with Borchers' data for the isotope shifts measured by Plimmer *et al.* [16] for two-photon excitation to the nearby $5p^5(^2P_{3/2})6p\ ^2[1/2]_0$ state.

The calculated K^* value is less than unity, which indicates a partial cancellation of the normal mass shift by a specific mass shift of comparable magnitude. The F^* value is of similar magnitude (and opposite sign) to that of certain s-p transitions [14], despite not directly involving any s electrons. Large values of F^* were previously observed in other transitions

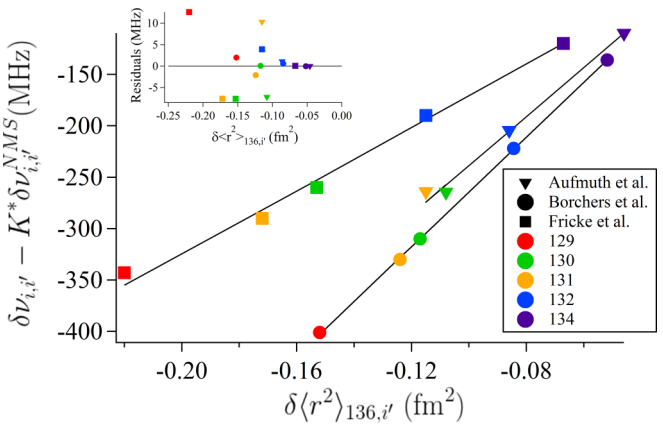

FIG. 3. Calculated field shifts vs $\delta\langle r^2\rangle$ for three published data sets [13,23,24]. Inset: residuals from the linear fit are smallest for Borchers' data.

which involve no s electrons [16,25,26]. It was surmised [16] that removing a $5p$ electron from the closed shell reduces the screening of inner s electrons and therefore increases the electron density at the nucleus.

We measured a photon count rate of $7.4(2) \times 10^8$ s^{-1} for the ^{132}Xe peak under the present conditions and correcting for the different APD sensitivities and fluorescence branching ratios of 823 nm and 895 nm [27]. The detection optics subtend a solid angle of 0.3 sr, limiting detection along the length of the excitation region. Previous works have calculated a cross section by assuming isotropic emission of LIF [28,29], but these values differ by an order of magnitude, with uncertainty due to nonradiative decay and possible excimer formation. In addition, we expect anisotropy in the observed fluorescence due to the effects of coherent on-axis emission as was previously observed [30]. A thorough calculation of the two-photon absorption cross section is beyond the scope of this paper.

In conclusion, we investigated the two-photon excitation of Xe for the $5p^5 6p(J = 2) \leftarrow 5p^6(J = 0)$ transition with the goal of developing a ^{129}Xe magnetometer. We have observed excitation spectra with well-resolved hyperfine structure and isotope shifts. We confirmed that the $F = 3/2$ and $F = 5/2$ excited levels of ^{129}Xe are well separated by 2216 MHz, which will allow us to detect the precession of polarized Xe atoms via excitation to the $F = 3/2$ level of this transition with a narrow linewidth laser system. The analysis of the isotope shift indicates that our own data support Borchers' reported values for the change in the nuclear radius-squared $\delta\langle r^2\rangle_{i,i'}$ for Xe isotopes ($i = 129 \sim 136$).

Our next steps are to obtain spectra at lower pressure and also to measure the dependence of such spectra on nuclear polarization and probe light polarization. Since at present the transition frequency accuracy is limited by the pressure shift, low-pressure measurements are necessary to determine the absolute transition frequency. The lower pressure is also crucial for the planned nEDM measurements at TRIUMF in order to avoid electric breakdowns due to the applied fields. The present photon counting rate predicts that the transition to the $F = 3/2$ level of ^{129}Xe can be detected at a signal-to-noise ratio of >10 with a 10 ms measurement of isotopically pure ^{129}Xe gas at 1 mTorr. This is sufficient to detect the precession of polarized ^{129}Xe with a field measurement accuracy of $\sim$pT. In order to reach $<10^{-27}e$ cm in the nEDM measurement, further improvement down to 30 fT field accuracy will be necessary, made possible by increasing the excitation power as well as improving the detection geometry. For our cavity geometry, constrained for other reasons, the beam focus was $60\,\mu\text{m} = w_o$. Reducing this would increase the signal by $1/w_o^2$ until the Rayleigh range becomes smaller than the capture region of the collection optics.

ACKNOWLEDGMENTS

We wish to thank A. Mills and P. Djuricanin for helpful discussions and technical assistance. This work was done under the auspices of the Center for Research on Ultra-Cold Systems (CRUCS). We acknowledge financial support from the Natural Sciences and Engineering Research Council of Canada (NSERC/CRSNG) and the Canada Foundation for Innovation (CFI). T.H. gratefully acknowledges support of Japan Society for the Promotion of Science (JSPS) Overseas Research Fellowships.

[1] R. Picker, Proceedings of the 14th International Conference on Meson-Nucleon Physics and the Structure of the Nucleon (MENU2016), JPS Conf. Proc. **13**, 010005 (2017).
[2] J. Pendlebury, S. Afach, N. Ayres, C. Baker, G. Ban, G. Bison, K. Bodek, M. Burghoff, P. Geltenbort, K. Green *et al.*, Phys. Rev. D **92**, 092003 (2015).
[3] J. Pendlebury, W. Heil, Y. Sobolev, P. Harris, J. Richardson, R. Baskin, D. Doyle, P. Geltenbort, K. Green, M. Van Der Grinten *et al.*, Phys. Rev. A **70**, 032102 (2004).
[4] T. Hayamizu, E. Altiere, E. Miller, J. Wienands, D. Jones, K. Madison, and T. Momose, http://meetings.aps.org/link/BAPS.2016.DNP.FJ.6.
[5] J. Kopecky *et al.* IAEA report, INDC(NDS)-362 (1997), https://www-nds.iaea.org/publications/indc/indc-nds-0362/.
[6] A. Kraft, H.-C. Koch, M. Daum, W. Heil, T. Lauer, D. Neumann, A. Pazgalev, Y. Sobolev, and A. Weis, EPJ Tech. Instru. **1**, 8 (2014).
[7] E. A. Alden, S. M. Degenkolb, T. E. Chupp, and A. E. Leanhardt, in *APS Division of Atomic, Molecular and Optical Physics Meeting Abstracts*, Vol. 56, No. 5 (APS, Ridge, 2011).
[8] A. K. Mills, Y.-F. Chen, K. W. Madison, and D. J. Jones, J. Opt. Soc. Am. B **26**, 1276 (2009).
[9] E. G. Jones, Proc. R. Soc. A **144**, 587 (1934).
[10] D. Jackson and M. Coulombe, Proc. R. Soc. A **335**, 127 (1973).
[11] W. Fischer, H. Hühnermann, G. Krömer, and H. J. Schäfer, Z. Phys. **270**, 113 (1974).
[12] W. L. Faust and M. McDermott, Phys. Rev. **123**, 198 (1961).
[13] W. Borchers, E. Arnold, W. Neu, R. Neugart, K. Wendt, G. Ulm (ISOLDE Collaboration), Phys. Lett. B **216**, 7 (1989).
[14] G. D'Amico, G. Pesce, and A. Sasso, Hyperfine Interact. **127**, 121 (2000).
[15] M. Suzuki, K. Katoh, and N. Nishimiya, Spectrochim. Acta, Part A **58**, 2519 (2002).
[16] M. Plimmer, P. Baird, C. Foot, D. Stacey, J. Swan, and G. Woodgate, J. Phys. B **22**, L241 (1989).
[17] R. Seiler, T. Paul, M. Andrist, and F. Merkt, Rev. Sci. Instrum. **76**, 103103 (2005).
[18] M. Kono, Y. He, K. G. Baldwin, and B. J. Orr, J. Phys. B **49**, 065002 (2016).
[19] G. Racah, Phys. Rev. **61**, 537 (1942).
[20] J. Paul, Y. Kaneda, T.-L. Wang, C. Lytle, J. V. Moloney, and R. J. Jones, Opt. Lett. **36**, 61 (2011).
[21] D. A. Steck, *Quantum and Atom Optics*, available online at http://steck.us/teaching (revision 0.12.0) (2017), p. 318.
[22] N. J. Stone, At. Data Nucl. Data Tables **90**, 75 (2005).
[23] P. Aufmuth, K. Heilig, and A. Steudel, At. Data Nucl. Data Tables **37**, 455 (1987).
[24] G. Fricke, C. Bernhardt, K. Heilig, L. Schaller, L. Schellenberg, E. Shera, and C. Dejager, At. Data Nucl. Data Tables **60**, 177 (1995).

[25] T. A. Paul and F. Merkt, J. Phys. B **38**, 4145 (2005).
[26] F. Brandi, I. Velchev, W. Hogervorst, and W. Ubachs, Phys. Rev. A **64**, 032505 (2001).
[27] H. Horiguchi, R. Chang, and D. Setser, J. Chem. Phys. **75**, 1207 (1981).
[28] T. D. Raymond, N. Böwering, C.-Y. Kuo, and J. W. Keto, Phys. Rev. A **29**, 721 (1984).
[29] S. Kröll and W. K. Bischel, Phys. Rev. A **41**, 1340 (1990).
[30] M. B. Rankin, J. P. Davis, C. Giranda, and L. C. Bobb, Opt. Comm. **70**, 345 (1989).